Hindawi
Advances in Civil Engineering
Volume 2018, Article ID 8190908, 8 pages
https://doi.org/10.1155/2018/8190908

Research Article

Stability Analysis Method for Rock Slope with an Irregular Shear Plane Based on Interface Model

Changqing Qi, Jiabing Qi, Liuyang Li, and Jin Liu

School of Earth Sciences and Engineering, Hohai University, Nanjing 210098, China

Correspondence should be addressed to Changqing Qi; qichangqing79@gmail.com

Received 27 October 2017; Revised 19 February 2018; Accepted 27 February 2018; Published 1 April 2018

Academic Editor: Giovanni Garcea

Landslide developed in rock mass usually has irregular shear plane. An approach for calculating distributed factor of safety of the irregular shear plane was put forward in this paper. The presented method can obtain not only the detailed stability status at any grid node of a complex shear plane but also the global safety of the slope. Thus, it is helpful to thoroughly understand the mechanism of slope failure. Comparing with the result obtained through the limit equilibrium method, the presented method was proved to be more accurate and suitable for stability analysis of rock slope with a thin shear plane. The stability of a potentially unstable rock slope was analyzed based on the presented method at the end of this paper. The detailed local stability, global stability, and the potential failure mechanism were provided.

1. Introduction

Landslide is one of the most severe geohazards threatening the interests of human [1, 2]. To prevent great losses of life and property, early hazard appraisal and assessment techniques needed to be implemented. Large landslides developed in rock mountains often have complex failure mechanism [3, 4]. The distributed safety along the sliding surface is as important as global safety in thoroughly understanding the failure behaviors of the slope. Hence, a convenient and practical approach to evaluate the stability of a slope should be developed which allows for the distributed safety along the sliding surface. Quantitative stability assessment method is useful in reducing the risk of disaster and mitigating the geohazardous damage. Despite the progress of simulation techniques, the use of the factor of safety (FOS) is still the most commonly adopted method in slope stability analysis. The wildly accepted definition of FOS is the ratio of shear strength of soil to shear stress required for equilibrium [4]. Among the various approaches to determine the FOS, limit equilibrium method and strength reduction method are the ordinary used methods [5–14]. These two methods are more convenient for 2D problem and regular slip surface. Some researchers have provided methods for three-dimensional slope stability analysis [15–18], but the obtained FOS was too large to use [4]. Furthermore, these methods can only obtain the global FOS of the slope. This is not enough for understanding the behavior of slope failure. The FOS may vary on different parts of the sliding surface [19].

The landslides developed in rock mass usually controlled by the combination of discontinuities. The separated part is often a 3D irregular geological body. The FOS at different parts of the separated surfaces must be addressed. A method for calculating the distributed FOS along the irregular sliding surfaces in rock slope was presented. On the basis of the definition of FOS and using the interface element model, FOS at any part of the sliding surface can be obtained. Then, the global FOS of the slope was given by the weighted average of shear strength to shear stress in the overall sliding direction, which can estimate the global stability of the slope.

2. Methods

The interface model of Flac^{3D} [20] was introduced to simulate the thin and weak shear plane. An interface is a connection face between two materials that is characterized by Coulomb sliding and/or tensile and shear bonding. The interface was discretized into triangular interface element. The interface node is located at the vertex of the element and

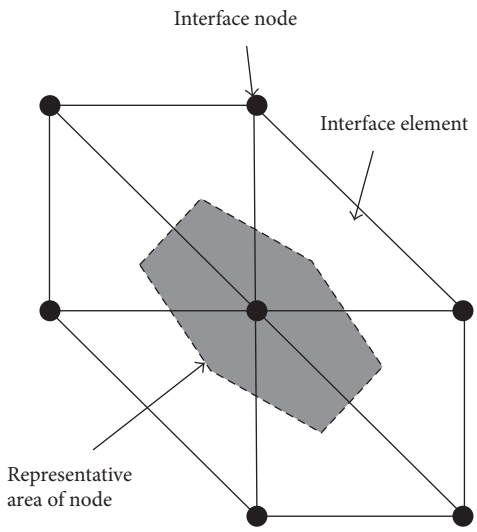

Figure 1: Interface element of Flac^{3D}.

has an associated representative area (Figure 1). The Coulomb shear strength criterion was employed to simulate the behavior of the interface. Flac^{3D} is an explicit finite difference program. The program adopts the explicit, Lagrangian calculation scheme and the mixed-discretization zoning technique in solving the dynamic equations. By assuming linear variations of the variable over finite space and time intervals, derivatives of a variable with respect to space and time are approximated by finite differences. The solution requires a number of computational timesteps to reach an equilibrium status. The normal and shear stress at any computational timestep $(t + \Delta t)$ on the representative area of a node can be obtained by

$$\begin{aligned} \sigma^{(t+\Delta t)} &= k_{\mathrm{n}} u_{\mathrm{n}} + \sigma_0, \\ \tau^{(t+\Delta t)} &= \tau^{t} + k_{\mathrm{s}} \Delta u_{\mathrm{s}}^{(t+1/2\Delta t)} + \tau_0, \end{aligned} \tag{1}$$

where u_{n} is the absolute normal penetration of the interface node into the target face, Δu_{s} is the incremental relative shear displacement vector, σ is the normal stress, τ is the shear stress, k_{n} is the normal stiffness, and k_{s} is the shear stiffness.

The normal stiffness k_{n} and the shear stiffness k_{s} were suggested to ten times the equivalent stiffness of the stiffest neighboring zone [20]:

$$k_{\mathrm{n}} = k_{\mathrm{s}} = \frac{10\,(K + 4/3G)}{\Delta z_{\min}}, \tag{2}$$

where K and G are the bulk and shear moduli of the softer side material and $\Delta z_{\min}$ is the smallest width of an adjoining zone of the softer side in the normal direction to the interface.

$$\begin{aligned} K &= \frac{E}{3\,(1 - 2\mu)}, \\ G &= \frac{E}{2\,(1 + u)}, \end{aligned} \tag{3}$$

where E is Young's modulus and μ is Poisson's ratio.

After obtaining the normal and shear stress, the FOS at any stress node can be given as follows based on the definition of FOS [5]:

$$f_{\mathrm{s}} = \frac{\tau_{\mathrm{u}}}{\tau} = \frac{c + (\sigma - p_{\mathrm{w}}) \times \tan\varphi}{\tau}, \tag{4}$$

where f_{s} represents the factor of safety at the grid node, τ_{u} represents shear strength, c is the cohesion, φ is the friction angle, and p_{w} is the pore pressure when below ground water table. f_{s} can be the referential index for stability analysis. It can give the safety status at any grid node of the slip surface.

Weighted with the area of the interface node, the global FOS of the shear plane can be given as follows:

$$F_{\mathrm{s}} = \frac{\sum_{i=1}^{n} \left((\sigma_i - p_{\mathrm{w}i}) \tan\phi_i \sin\delta_i \times A_i + cA_i \right)}{\sum_{i=1}^{n} \left((\tau_i \times \cos\delta_i) \times A_i \right)}, \tag{5}$$

where F_{s} is the global FOS of sliding surface, n is the node on the interface, A_i is the representative area of the ith node, and δ_i is the angle between the shear vector and the project of the overall shear direction on the representative area of the ith node.

3. Method Verification

The limit equilibrium method is the widely used and accepted slope stability analysis method. It was adopted to verify our method for a unit width slope with a thin-layer shear plane. The slope is 43 m in horizontal and 32.5 m in elevation. The shear plane was set to be 5 cm in the limit equilibrium model and simulated as an interface in the numerical model. The properties of the soils are given in Table 1.

The software Slide 6.0 [21] was used, and the Bishop method was selected in limit equilibrium analysis. The noncircular surface type was chosen, and the block search method was adopted. The geometric model and the result determined by the Bishop method are shown in Figure 2. The global FOS along the given shear plane is 1.109.

Figure 3 shows the numerical model and the result obtained by the method presented in this paper. The shear stiffness and normal stiffness obtained from (2) are both 3.2×10^{10} Pa/m. The smallest width of the adjoining zone in the normal direction to the interface is 0.5 m. The global FOS obtained by our method is 1.101. The error between the two methods is only 0.7%. It proved that the presented method has high accuracy and is acceptable in slope stability analysis. Figure 3 also shows the distribution of the FOS along the shear plane. The FOS on the back scarp of the shear plane is lower. Actually, most area of the back scarp has a FOS lower than 1.0, indicating a potential instability status of the back scarp. The FOS on the bottom sliding surface increases from the back scarp to the toe, which gives rise to a slide resistance near the toe. This phenomenon coincides with the common mechanical characteristics of a slope with a weak shear plane [22–24].

4. Application and Implementation

The presented method was used for stability analyses of a potentially unstable rock slope in Sichuan Province,

Table 1: Properties of soils used in the verification model.

Soil type	Unit weight (kN/m^3)	Young's modulus (GPa)	Poisson's ratio	Cohesion (kPa)	Friction angle (°)
Unstable slope	20.5	1.0	0.35	40	30
Shear plane	20.0	0.2	0.35	15	24
Bedrock mass	24.0	10	0.3	70	35

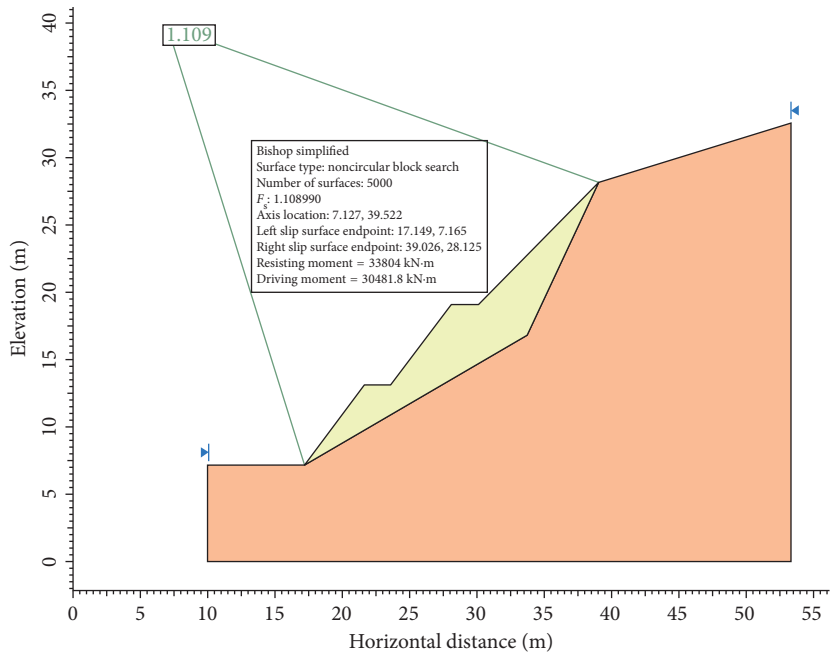

Figure 2: Limit equilibrium result using the Bishop method of the verification model.

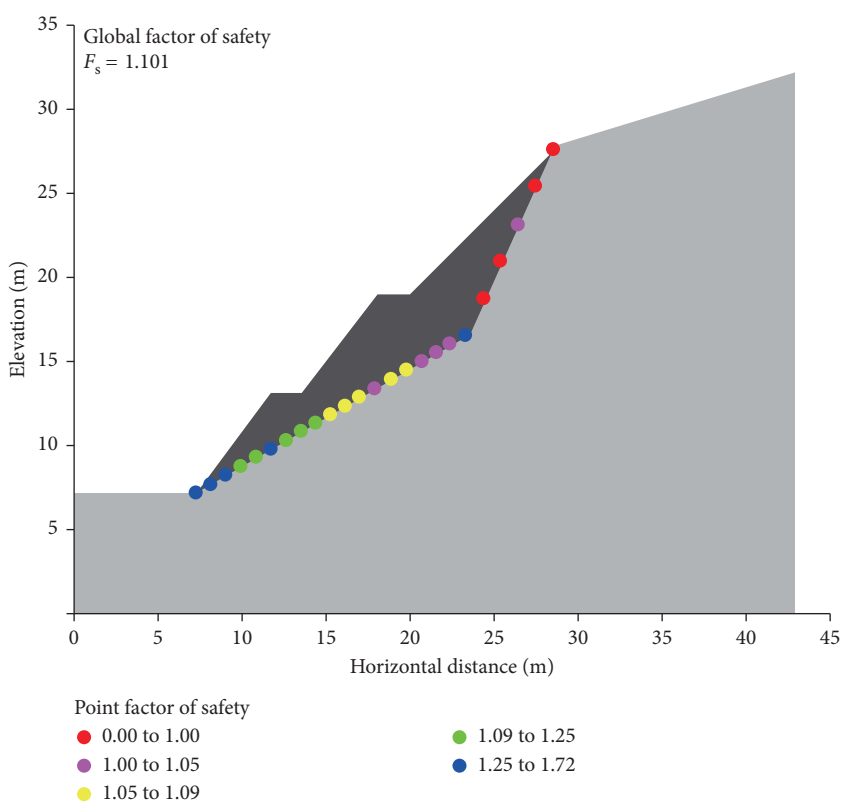

Figure 3: Result obtained by the presented method of the verification model.

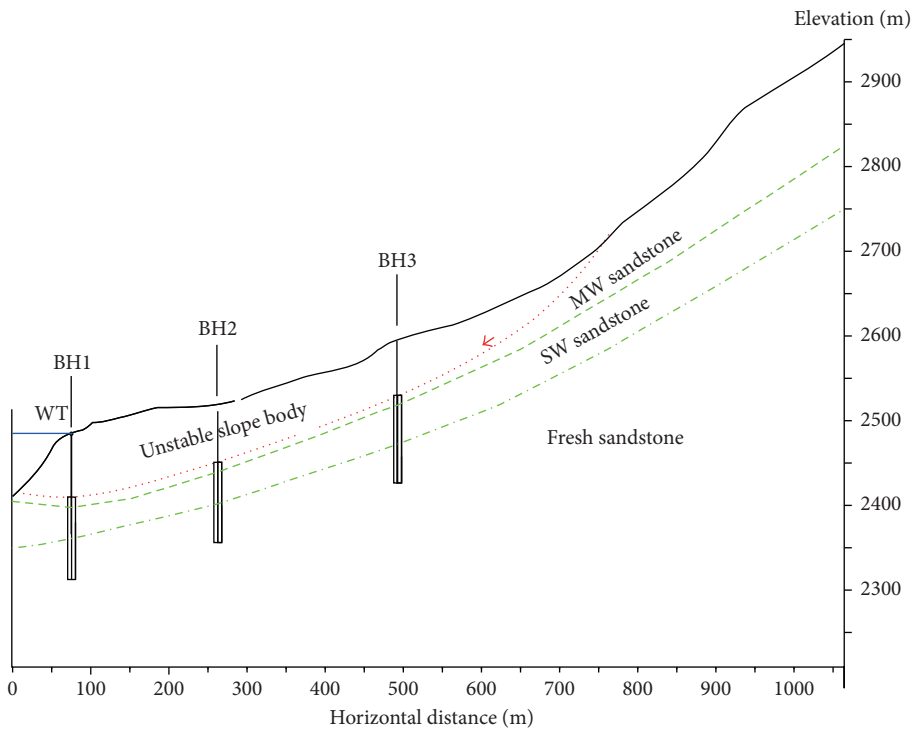

Figure 4: Longitudinal section of the studied slope (MW, moderately weathered sandstone; SW, slightly weathered sandstone; WT, water table).

Table 2: Physical and mechanical properties of relevant materials.

Soil type	Natural weight (kN/m^3)	Saturated weight (kN/m^3)	Young's modulus (GPa)	Poisson's ratio	Cohesion (kPa)	Friction angle (°)
Potential unstable slope body	20.5	22.6	0.5	0.35	40	30
Shear plane	19.0	21.0	NA	0.35	15	22.5
MW sandstone	24.0	25.5	10	0.3	70	35
SW sandstone	25.0	NA	35	0.2	300	45
Fresh sandstone	27.0	NA	45	0.2	800	50

Southwest China. The potentially unstable slope, located at the flank of the Yalong River, has a total volume of about 800 million·m^3. It covers upslope from 2380 m to 2730 m a.s.l. (Figure 4). The shear plane was explored by boreholes. It developed from the discontinuities of the rock mass. The studied slope will be in the reservoir of a proposed hydraulic power station. The toe will be immersed in the dammed water. So the stability and potential sliding mechanism of the slope need to be studied in detail.

The slope can be distinguished as four geologic layers from the borehole data. The top unstable slope body, with a maximum thickness of 80.0 m, overlies a layer of heavily weathered sandstone approximately 15 m thick. A moderately weathered sandstone layer underlies the heavily weathered sandstone and extends to a depth of 140–145 m. The bottom bedrock is the fresh sandstone. The physical and mechanical properties of the relevant materials are shown in Table 2. As suggested in some previous studies [25, 26], the shear strength parameters used in the analysis are opportunely reduced by a factor of 0.75 for the potentially unstable soil mass and the failure surface, and 0.85 for the bedrock, to account for the influence of moisture.

The shear plane was considered as an interface in the numerical model. The shear stiffness and normal stiffness obtained from (2) are both 2×10^9 Pa/m. The smallest width of the adjoining zone in the normal direction to the interface is 4.0 m. The three-dimensional numerical grids of the slope and the interface are shown in Figure 5.

5. Result Analyses

5.1. Slope Stability at Present. Figure 6 gives the distribution of normal stress and shear stress on the interface. It can be seen from Figure 6 that the normal stress mainly concentrates on the lower part of the interface. The maximum normal stress appears at the transition area where the slope of the shear plane changes from steep to gentle. The maximum normal stress is about 1.4 MPa. The normal stress approaches to zero near the border of the shear plane. On contrary to the distribution of normal stress, the shear stress

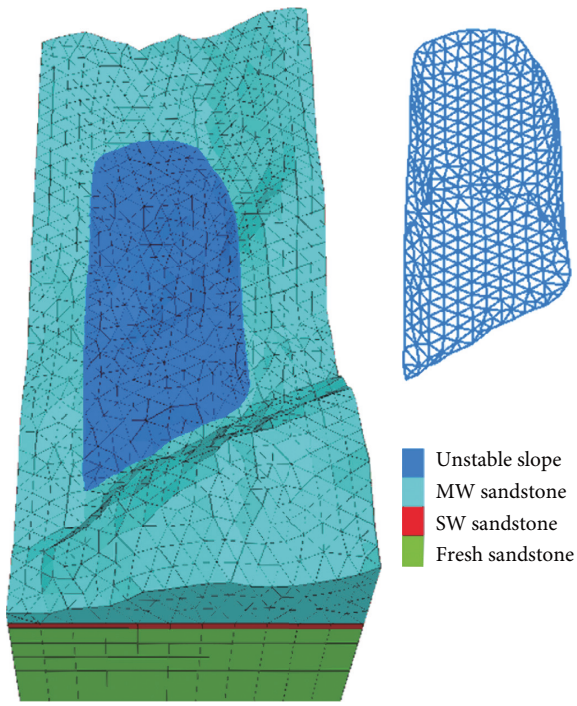

Figure 5: Numerical grid of the slope and the interface.

concentrates mainly on the upper part of the shear plane, indicating a large sliding potential of the upper slope. The shear stress is also small near the border and at the areas with gentle slope angles.

The FOS on the shear plane was obtained from (4). Figure 7 shows the distribution of the FOS. It indicates that there are several small areas near the border of the shear plane where the factors of safety are smaller than 1.0. Most portion of the shear plane has factors of safety ranging from 1.0 to 1.5, indicating a relatively stable condition. At the lower-middle part and the toe, there are some areas where the factors of safety are above 2.0.

Figure 8 illustrates the nodal FOS on the shear plane. It can give more comprehensive information about the stability of the slope. There are sporadic points where the factors of safety are below 1.0 (red point), indicating there will be cracks or breaks near the border of the unstable body. The FOS increases downslope along the shear plane. At the upper one-third of the shear plane, nearly all the nodal factors of safety are less than 1.05. It can be concluded that the head of the slope body has a large instability potential. The top one-third of the slope lacks sufficient ability of self-stability and poses a residual thrust force on the lower part. At the middle one-third of the shear plane, most nodal factors of safety are between 1.05 and 1.5, implying a relatively stable state. At the lower one-third of the shear plane, there are lots of points with factors of safety larger than 1.5. The middle and lower parts of slope with higher FOS act as sliding resistance and provide necessary safety capacity for the stability of the slope. The global FOS of the slope obtained from (5) is 1.23. This value proves that the entire slope is more stable at present.

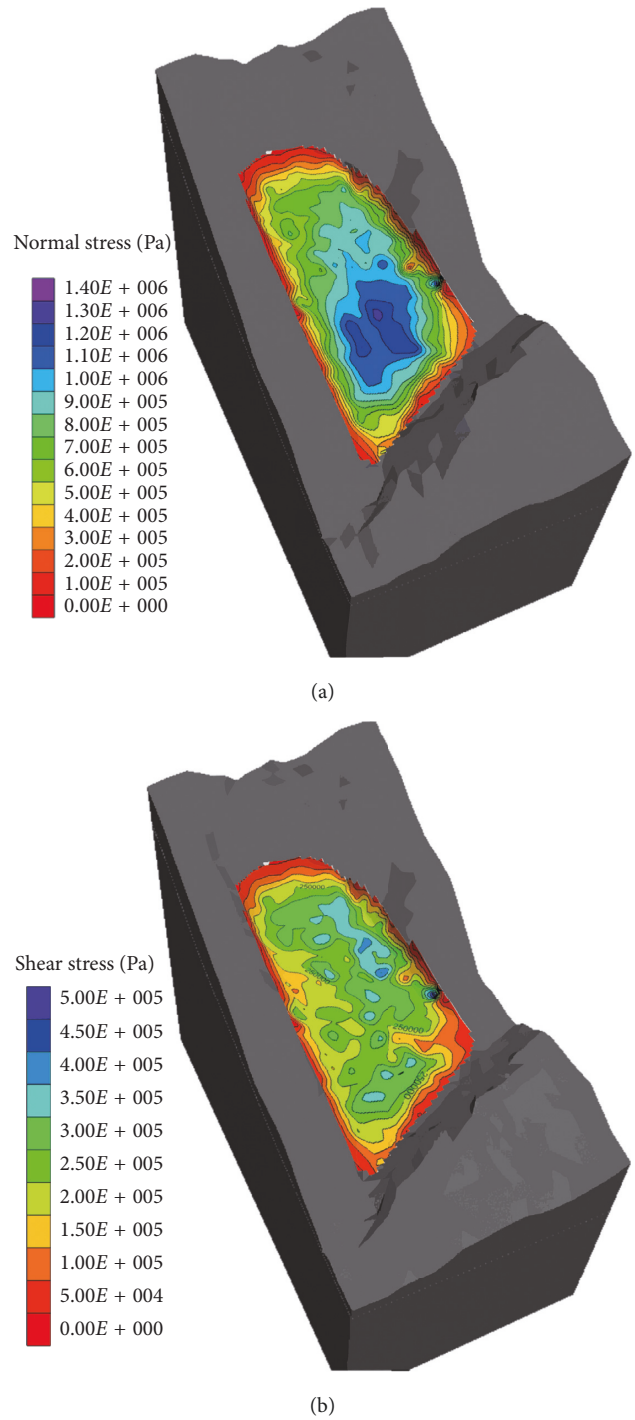

Figure 6: Distribution of normal stress (a) and shear stress (b) at the natural state.

5.2. Slope Stability after Impounded. The distribution of normal and shear stresses after the proposed reservoir impounded is given in Figure 9. The maximum value of the normal stress reduces a little at the vicinity of the water level when the proposed reservoir is in operation. But the shear stress below water level increases greatly comparing with the natural condition. The large shear stress near the toe increases the risk of slope failure.

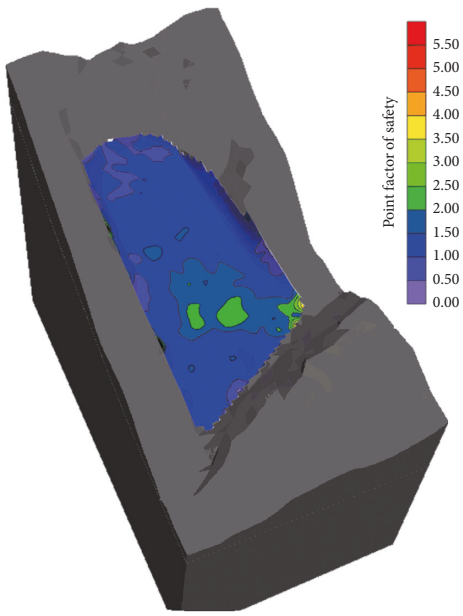

Figure 7: Distribution of factor of safety at the natural state.

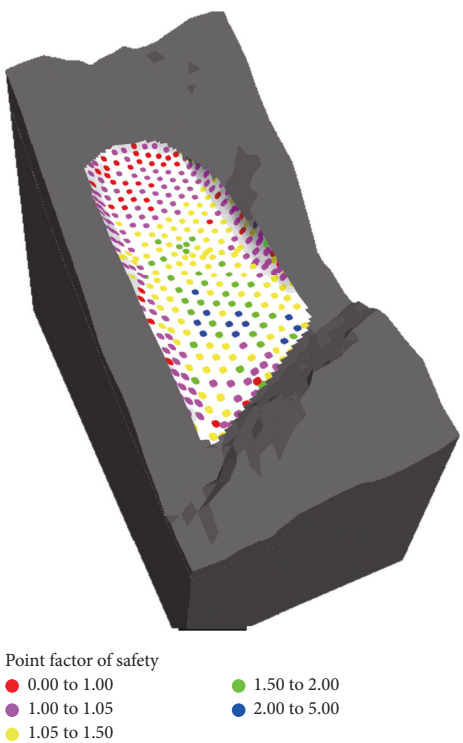

Figure 8: Point factor of safety at the natural state.

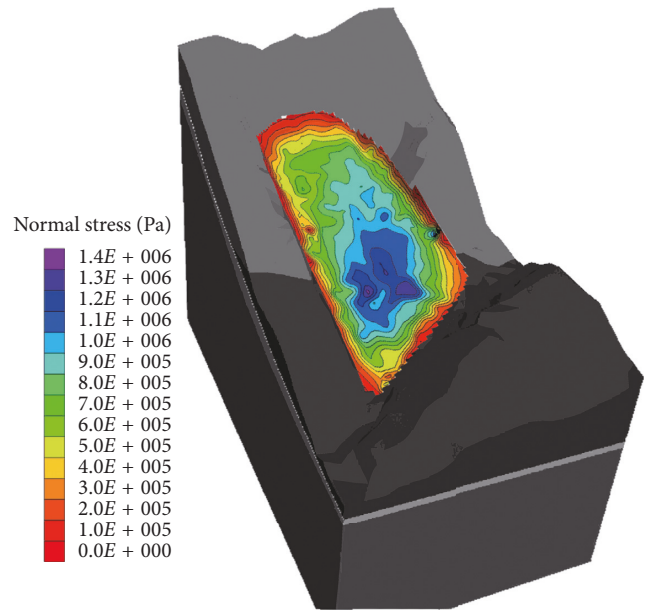

(a)

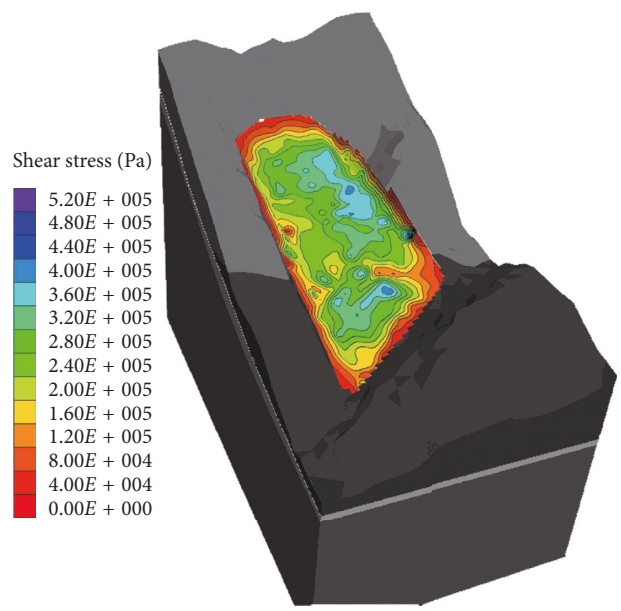

(b)

Figure 9: Distribution of normal stress (a) and shear stress (b) after impounded.

Figure 10 exhibits the distribution of FOS on the shear plane after the proposed reservoir impounded. It can be seen that there are more unstable areas (with FOS < 1.0). This phenomenon is more obvious at the toe of the slope. The factors of safety on a majority of areas are below 1.5, and only very small areas have factors of safety larger than 2.0.

Figure 11 demonstrates the nodal FOS on the shear plane after reservoir impounded. It reveals that the FOS decreases at nearly all the interface nodes. At the lateral borders, more unstable points appear and the distribution of unstable points approaches inward. At the top one-third and the toe of the shear plane, nearly half of the nodes are unstable. It suggests that the top one-third slope will throw more residual thrust on the lower part, and there may be failures at the toe of the slope. There are several points with factors of safety above 1.5 and only one point with a FOS larger than 2.0. Thus, the sliding resistance of the lower part will reduce. The global FOS has a clearly reduction and is now 1.09. The slope is only slightly stable and cannot ensure the safety of

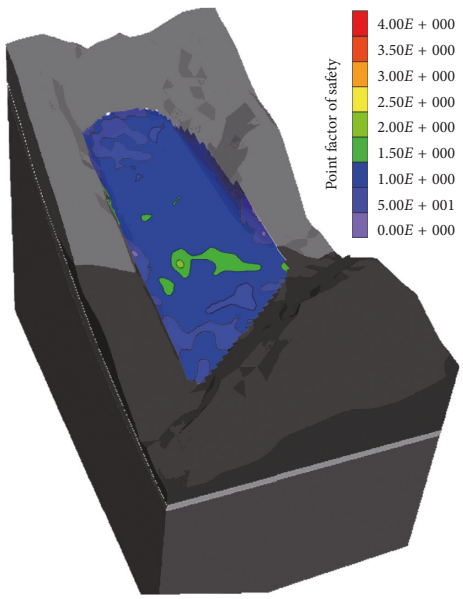

Figure 10: Distribution of factor of safety after impounded.

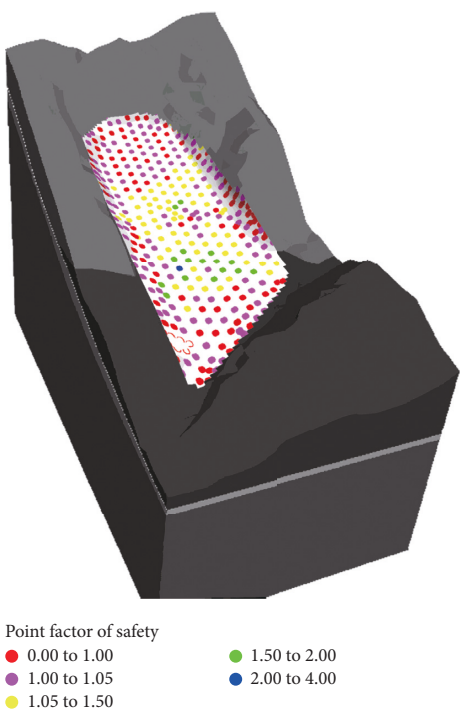

Figure 11: Point factor of safety after impounded.

the project in the view of engineering. The lower part of the slope must be reinforced.

6. Conclusion

A method for distributed FOS calculation of irregular three-dimensional shear plane was presented in this paper. This method is more suitable for stability assessment of rock mass slope with thin-layer shear zone. The presented method was first verified and implemented and then was applied in stability assessment of a high-focused rock slope. The research leads to the following conclusions:

(1) The presented method can give the distribution and global FOS of irregular shear plane. It is useful in sliding mechanism understanding and failure mode distinguishing, as well as global stability evaluation. Comparing with the traditional FOS analysis method, the presented method can give more direct and detailed reference for landslide disaster mitigation.

(2) The error of global FOS between the presented method and Bishop method is only 0.7% for a typical rock slope. The proposed method was proved to be accurate and suitable in stability analysis of rock slope with thin shear planes.

(3) The stability of a practical rock slope was analyzed using the present method. The global FOS of the slope is 1.23 at the natural condition. The top one-third part of studied slope has a sliding potential and poses residual thrust on the lower part. The one-third part near the toe of the slope is more stable and provides sliding resistance to the entire slope. The entire slope is currently more stable.

(4) The global and nodal factors of safety both decrease when the toe of the slope was immersed in the proposed damming water. The global factor of safety reduces to 1.09, and some areas below the water level become unstable. Considering the elevated risk of landslide hazards and the threaten to the engineering infrastructure of the proposed hydropower station, slope reinforcement measures, such as pile-anchor support, surface water control, or material cutting, should be performed.

Conflicts of Interest

The authors declare that they have no conflicts of interest.

Acknowledgments

The authors greatly appreciate the support provided by the National Natural Science Foundation of China (no. 41272328) and the Fundamental Research Funds for the Central Universities (no. 2015B16514).

References

[1] F. C. Dai, C. F. Lee, and Y. Y. Ngai, "Landslide risk assessment and management: an overview," *Engineering Geology*, vol. 64, no. 1, pp. 65–87, 2002.

[2] Z. Y. Chen, X. M. Meng, Y. P. Yin, T. Dijkstra, M. Winter, and J. Wasowski, "Landslide research in China," *Quarterly Journal of Engineering Geology and Hydrogeology*, vol. 49, no. 4, pp. 279–285, 2016.

[3] D. Stead, E. Eberhardt, and J. Coggan, "Developments in the characterization of complex rock slope deformation and failure using numerical modelling techniques," *Engineering Geology*, vol. 83, no. 1–3, pp. 217–235, 2006.

[4] C. Q. Qi, J. M. Wu, J. Liu, and D. P. Kanungo, "Assessment of complex rock slope stability at Xiari, southwestern China," *Bulletin of Engineering Geology and the Environment*, vol. 75, no. 2, pp. 537–550, 2016.

[5] J. Duncan, "State of the art: limit equilibrium and finite-element analysis of slopes," *Journal of Geotechnical Engineering*, vol. 122, no. 7, pp. 577–596, 1996.

[6] A. W. Bishop, "The use of the slip circle in the stability analysis of slopes," *Géotechnique*, vol. 5, no. 1, pp. 7–17, 1955.

[7] N. R. Morgenstern and V. E. Price, "The analysis of the stability of general slip surfaces," *Géotechnique*, vol. 15, no. 1, pp. 79–93, 1965.

[8] E. Spencer, "A method of analysis of the stability of embankments assuming parallel interslice forces," *Géotechnique*, vol. 17, no. 1, pp. 11–26, 1967.

[9] N. Janbu, "Slope stability computations," in *Soil Mechanics and Foundation Engineering*, The Technical University of Norway, Trondheim, Norway, 1968.

[10] O. C. Zienkiewicz, C. Humpheson, and R. W. Lewis, "Associated and nonassociated visco-plasticity and plasticity in soil mechanics," *Géotechnique*, vol. 25, no. 4, pp. 671–689, 1975.

[11] D. J. Naylor, "Finite elements and slope stability. Numerical methods in geomechanics," in *Proceedings of the NATO Advanced Study Institute*, pp. 229–244, Lisbon, Portugal, 1981.

[12] E. M. Dawson, W. H. Roth, and A. Drescher, "Slope stability analysis by strength reduction," *Géotechnique*, vol. 49, no. 6, pp. 835–840, 1999.

[13] T. Matsui and K. C. San, "Finite element slope stability analysis by shear strength reduction technique," *Soils and Foundations*, vol. 32, no. 1, pp. 59–70, 1992.

[14] G. H. Sun, S. G. Cheng, W. Jiang, and H. Zheng, "A global procedure for stability analysis of slopes based on the Morgenstern-Price assumption and its applications," *Computers and Geotechnics*, vol. 80, pp. 97–106, 2016.

[15] P. Anagnosti, "Three dimensional stability of fill dams," in *Proceedings of the 7th International Conference on Soil Mechanics and Foundation Engineering*, Rotterdam, Netherlands, 1969.

[16] R. B. Seed, J. K. Mitchell, and H. B. Seed, "Kettlemen Hills waste landfill slope failure, II: stability analysis," *Journal of Geotechnical Engineering*, vol. 116, no. 4, pp. 669–690, 1990.

[17] A. Troncone, E. Conte, and A. Donato, "Two and three-dimensional numerical analysis of the progressive failure that occurred in an excavation-induced landslide," *Engineering Geology*, vol. 183, pp. 265–275, 2014.

[18] D. V. Griffiths and R. M. Marquez, "Three-dimensional slope stability analysis by elasto-plastic finite elements," *Géotechnique*, vol. 57, no. 6, pp. 537–546, 2007.

[19] A. K. Chugh, "Variable factor of safety in slope stability analysis," *Géotechnique*, vol. 36, no. 1, pp. 57–64, 1986.

[20] Itasca Consulting Group Inc., *FLAC3D-Fast Lagrangian Analysis of Continua in 3 Dimensions, Version 5.0*, ICG, Minneapolis, MN, USA, 2012.

[21] Rocscience Inc., *SLIDE Version 6.0–2D Limit Equilibrium Slope Stability Analysis*, Rocscience Inc., Toronto, ON, Canada, 2016.

[22] E. Conte, A. Donato, and A. Troncone, "A simplified method for predicting rainfall-induced mobility of active landslides," *Landslides*, vol. 14, no. 1, pp. 35–45, 2017.

[23] S. Leroueil, J. Vaunat, L. Picarelli, J. Locat, R. Faure, and H. Lee, "A geotechnical characterization of slope movements," in *Proceedings of the 7th International Symposium on Landslides*, vol. 1, pp. 53–74, Trondheim, Norway, June 1996.

[24] J. Corominas, J. Moya, A. Ledesma, J. A. Rius, J. A. Gili, and A. Lloret, "Monitoring of the Vallcebre landslide, Eastern Pyrenees, Spain," in *Proceedings of the International Symposium on Slope Stability Engineering*, pp. 1239–1244, Shikoku, Japan, November 1999.

[25] H. H. Wu and Z. J. Dong, "An approach to the geotechnical parameters c and φ for landslides in the Yangtze Gorges Reservoir Region, Chongqing," *Acta Geologica Sichuan*, vol. 29, no. 2, pp. 207–212, 2009, in Chinese.

[26] Y. J. Dong, Z. G. Zheng, Z. Q. Zhao et al., "Experimental study on the decrease regularity of the strength parameters of slip soil because of the influence of moisture," *Journal of North China University of Water Resources and Electric Power*, vol. 37, no. 2, pp. 83–86, 2016, in Chinese.